Applied Mathematical Modelling 40 (2016) 8592–8604

Contents lists available at ScienceDirect

Applied Mathematical Modelling

journal homepage: www.elsevier.com/locate/apm

A three dimensional simulation of a rubber curing process considering variable order of reaction

Mohammad-Reza Erfanian[a], Morteza Anbarsooz[b], Mohammad Moghiman[a,*]

[a] Mechanical Engineering Department, Ferdowsi University of Mashhad, Mashhad, Iran
[b] Mechanical Engineering Department, Quchan University of Advanced Technology, Quchan, Iran

ARTICLE INFO

Article history:
Received 17 September 2015
Revised 7 May 2016
Accepted 18 May 2016
Available online 25 May 2016

Keywords:
Cure process
Rubber
Optimum Curing time
Rheometry

ABSTRACT

Calculating the optimum curing time for thick molded rubbery parts is an important challenge in the rubber industry. This presented work is focused on the development of a computational technique for numerical simulation of the rubber vulcanization process in injection molding machines that can be used as a method for determining the best curing time of the final product. The main innovation of the work is introducing a kinetics model with variable order of reaction which enhances the accuracy of the calculated optimum curing time, especially in three-dimensional complex rubber articles. The method is used for simulation of the injection molding process of an automotive rubber part, containing both the mold filling and the cure reaction processes. The numerical predictions of the mold filling time and the curing time are compared with those of experiments, which confirmed the accuracy and capability of the proposed model.

1. Introduction

Rubber is widely used in various applications, from tires to flexible tubing or absorbing systems, to mention just a few applications. They are favored when, in contrast to other engineering materials, their stronger attributes are needed and, at the same time, their highly deformable characteristics are desirable [1]. However, raw rubber is very soft with low mechanical properties. It must be cured in a mold which is called the vulcanization process. Following the vulcanization process, the compound which is made up of uncured rubber and curing agents, fills the mold cavity during the injection cycle and is heated up to a temperature at which the cure reaction starts. During the cure, an irreversible reaction takes place, leading to a three-dimensional molecular network, and as a result, the weak material is converted into a very strong elastic product [1]. Obviously, the curing process specifications such as the curing time and curing temperature have strong impacts on the quality and mechanical properties of the final product [2].

Using experimental techniques to determine the required curing time for a rubber article to reach certain mechanical properties, is a time-consuming and expensive procedure. As a result, numerical solutions have been widely used in the rubber industry, following the development of computers and CAE tools. A comprehensive review on the historical background of the development of these techniques are presented by Ghoreishy [2] and hence, they are not repeated here.

Various kinetic models have been used to describe the cure behavior of rubber. Generally, these models are divided into two main categories; mechanistic kinetic models and empirical models [3]. Mechanistic kinetic models attempt to quantify

* Corresponding author. Tel.: +985138805091; fax: +985138806055.
E-mail address: moghiman@um.ac.ir (M. Moghiman).

http://dx.doi.org/10.1016/j.apm.2016.05.024
S0307-904X(16)30274-8/

the balance of chemical species involved in the curing reaction. Due to their complexity and the need to the knowledge of the underlying chemistry [4], these models have not been accepted as appropriate models for numerical simulations [3]. On the other hand, the empirical models or regression models ignore the chemical details of the cure system and fit the data to a mathematic functional form where the constants of the model are determined based on experimental procedures such as rheometry [4]. Some numerical studies that have applied empirical models in their simulations are reviewed below.

Ghoreishi and Naderi [5] developed a finite element model for the simulation of the rubber curing process in a mold. They used the kinetic model proposed by Kamal and Sourour [6] which has shown an acceptable agreement with the experimental data. Their investigations for a truck tire curing process also revealed that neglecting the heat transfer in one direction would produce significant errors in calculating the temperature fields and extends of the cure reaction [7]. Arillaga et al. [3] simulated the injection molding process for relatively simple geometries with uniform thickness using the Moldflow Software. This software has also been employed by Ramorino et al. [8] to perform a three-dimensional finite element simulation for the injection molding process of a rubber compound. Leroy et al. [9] presented a cure kinetic model predicting induction, main vulcanization and reversion stages and modeled the cure process for a sample test which had a uniform thickness. Rafei et al. [10] developed a numerical code to study the curing process of a simple rubber article in a mold using unstructured meshes. They also considered the thermal contact resistance between the rubber and the mold in their simulations. Their results demonstrated that the Kamal and Sourour [10] model fails to precisely describe the cure behavior especially at the early stages of the cure reaction and also at the non-isothermal conditions [10]. As a result, they introduced a modified version of that model which enhanced the accuracy of the results. They used the values of the state-of-cure at the initial and final stages of the reaction in their modified model.

The main motivation of the current study is to present a new modification to the Kamal and Sourour kinetic model. In the modified model, the model's order of reaction is no longer a constant, but it is a function of temperature. In order to verify the performance of the modified model, the injection molding process for an automotive rubber part, containing both the mold filling and the cure reaction processes, is studied numerically using the Fluent software. The new kinetic model is introduced into the Fluent 6.3.26 [11] software using a new User-Defined-Function (UDF) developed in C program. In order to determine the non-Newtonian fluid model constants, viscometry tests are performed. Rheometry tests are employed to determine the curing parameters of the kinetic model. Non-isothermal Differential Scanning Calorimetry (DSC) tests are also carried out at different temperatures to determine the temperature dependent specific heat of rubber. Mechanical compression tests are performed on the rubber component at different times of the curing process to determine the best curing time. The results of the numerical simulations with the Kamal kinetic model and the one modified in the current study are compared with the experimental results and the modified model has shown a better agreement with experimental data.

2. Mathematical modeling

2.1. Governing equations

Computational Fluid Dynamics (CFD) relies on solving conservation equations of mass, momentum and energy. These equations in a 3D Cartesian coordinate system are given below:

2.1.1. Continuity equation

$$\frac{\partial \rho}{\partial t} + \nabla.(\rho \vec{V}) = 0 \tag{1}$$

where ρ is the fluid density and $\vec{V}$ is the velocity vector.

2.1.2. Momentum conservation equation

$$\frac{\partial}{\partial t}(\rho \vec{V}) + \nabla.(\rho \vec{V}\vec{V}) = -\nabla p + \nabla.(\bar{\bar{\tau}}), \tag{2}$$

where p is the static pressure and τ is the viscous stress tensor. For a non-Newtonian fluid, the shear stress can be written as:

$$\bar{\bar{\tau}} = \mu(\nabla \vec{V} + \nabla \vec{V}^T), \tag{3}$$

where μ is the shear viscosity.

The non-Newtonian power law viscosity model, which has provided satisfactory predictions for rubber simulations, is applied in the present simulations. The model is given by Khor et al. [12]:

$$\mu = A(\dot{\gamma})^{B-1} \exp\left(\frac{T_0}{T}\right) \tag{4}$$

where A is a measure of the average viscosity of the fluid (the consistency index), $\dot{\gamma}$ is the shear rate, B is a measure of the fluid deviation from Newtonian (the power-law index), T is the temperature and T_0 is a reference temperature.

2.1.3. Energy conservation equation

$$\frac{\partial}{\partial t}(\rho E) + \nabla.(\vec{V}(\rho E + p)) = \nabla(k\nabla T + (\bar{\bar{\tau}}.\vec{V})) + S_h \tag{5}$$

where E is the specific energy, k is the thermal conductivity and S_h is the source term which consists of the chemical reactions heat release per unit volume and is a function of both the state-of-cure and the temperature [5,13].

2.1.4. Tracking the rubber front

The tracking of the interface between the rubber and air phases is carried out by the solution of a continuity equation for the volume fraction of the rubber phase. For the rubber phase, this equation can be written as [14]:

$$\frac{\partial}{\partial t}(f_a\rho_a) + \nabla \cdot (f_a\rho_a\vec{V}) = 0,$$

where f_a and ρ_a are the rubber volume fraction, respectively. The volume fraction of air can be calculated from the following equation:

$$f_b = 1 - f_a$$

where f_b is the air volume fraction.

2.2. Cure reaction kinetics

As discussed in the Section 1, the use of mechanistic kinetic models in the numerical simulations is usually difficult due to the complexity of the chemistry [3,4]. On the other hand, empirical kinetic models are regression models that fit the experimentally measured data to a particular functional form. These models have constants which are estimated from experimental data using non-linear regressions. In this study, the empirical kinetic model proposed by Kamal and Sourour [5,10] which is widely used in rubber curing problems is employed. This model is given by:

$$\alpha = \frac{k(t - t_i)^n}{1 + k(t - t_i)^n} \tag{6}$$

where α is the state-of-cure (or degree of cure) and its value goes between 0 (uncured rubber) and 1 (completely cured rubber), k is the temperature-dependent rate constant, n is the order of reaction and t_i is the induction time determined from the recorded data during the isothermal MDR tests (Section 4.2) at each temperature. During the induction time, the state of cure (α) remains zero because no chemical reaction takes place inside the rubber. The induction time (t_i) has Arrhenius-type temperature dependence [15]:

$$t_i = t_0 \exp\left(\frac{T_0}{T}\right) \tag{7}$$

where t_0 and T_0 are material dependent constants. In the non-isothermal case, induction time is implicitly expressed by an integral equation [15]:

$$\bar{t} = \int_0^t \frac{dt}{t_i(T)} \tag{8}$$

where t_i (T) is the isothermal induction time described by Eq. (7). When $\bar{t}$ attains a value equal to 1, the cure reaction has started and the upper limit of this integral (t) is considered as the non-isothermal induction time.

Referring to Eq. (6), the parameter k can be described by Arrhenius-type temperature dependence of the form [5,16]:

$$k = k_0 exp\left(\frac{-E}{RT}\right) \tag{9}$$

where k_0 is a material dependent constant, E is the activation energy and R is the universal gas constant. Using the non-linear curve fitting from experimental data, the constants of the kinetic model will be determined which are given in the Experiments Section.

2.3. User subroutine development

The state of cure is the basic feature related with the modeling of rubber curing processes that cannot be taken into account with standard options in Fluent. Therefore, it is necessary to add an extra subroutine to the Fluent solver as a user defined function (UDF), that is written in the C programming language. The flowchart of the UDF code and its interaction with the principal processor is shown in Fig. 1.

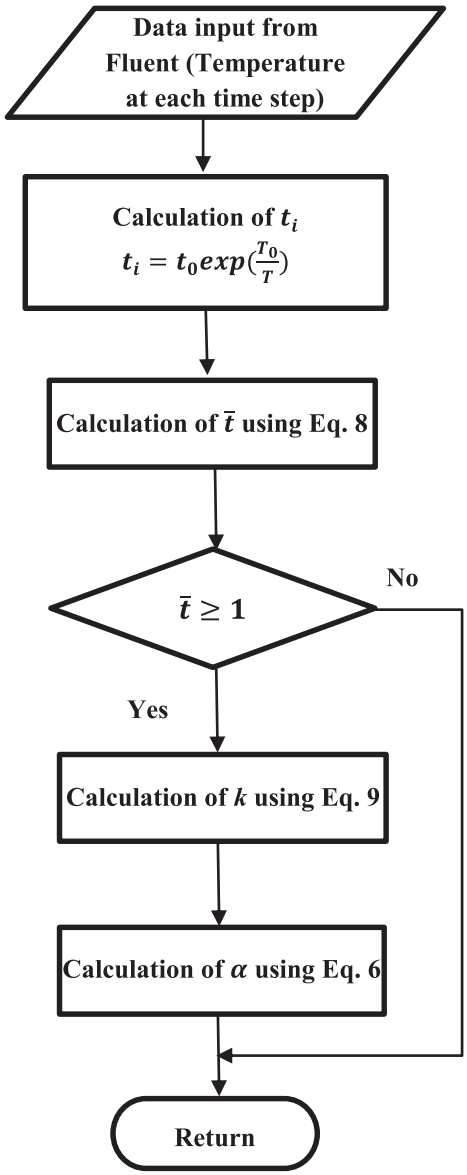

Fig. 1. Flow chart of curing UDF for the rubber.

3. Computational model

3.1. Model geometry, mesh generation and numerical method

The geometry of the three-dimensional model and the distribution of the generated grid inside the computational domain are shown in Figs. 2 and 3, respectively. An unstructured grid using tetrahedral elements is considered for the computational domain using Gambit 2.3 mesh generation software. The quality of the generated grid is ensured by checking the skewness of the cells. The grid size that represented mesh-independent results corresponds to 1,295,306 cells in the domain. The given governing equations have been solved using the commercial CFD software, Fluent 6.3.26, for an automotive rubber part. The software uses a control-volume-based technique to convert the governing equations to algebraic equations that can be solved numerically [11]. The Semi-Implicit Method for Pressure-Linked Equations (SIMPLE) type segregated algorithms are used for the velocity-pressure coupling and overall solution procedure. Momentum, volume fraction and energy conservation equations are solved using a first-order upwind implicit scheme. Also due to transient nature of the cure process, the governing equations are discretized in time. Temporal discretization involves the integration of every term in the differential equations over a time step [11].

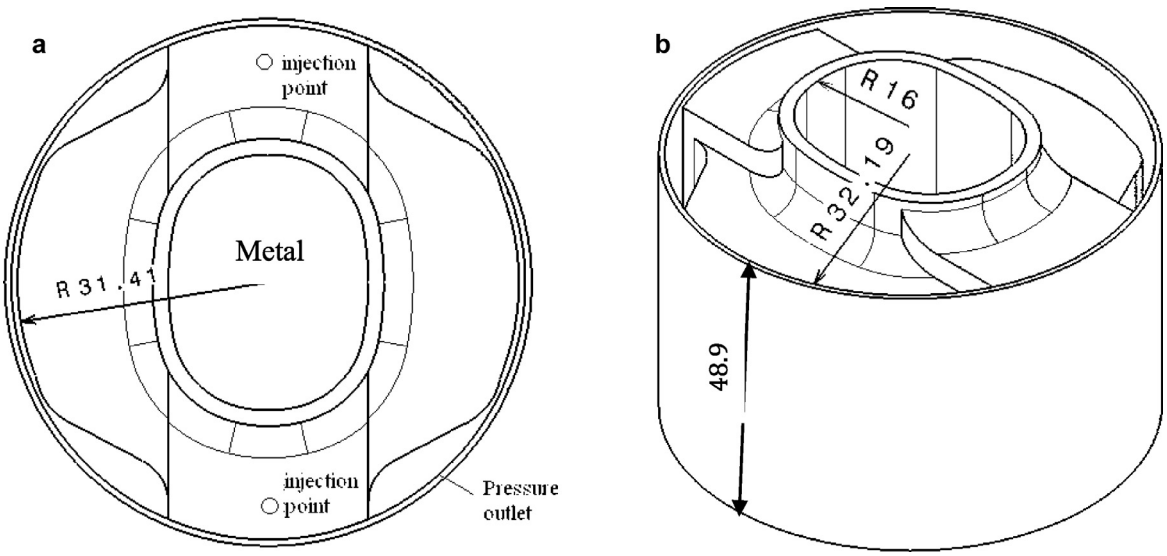

Fig. 2. Geometry dimensions (in mm) of the model, (a) Top view and (b) Isometric view.

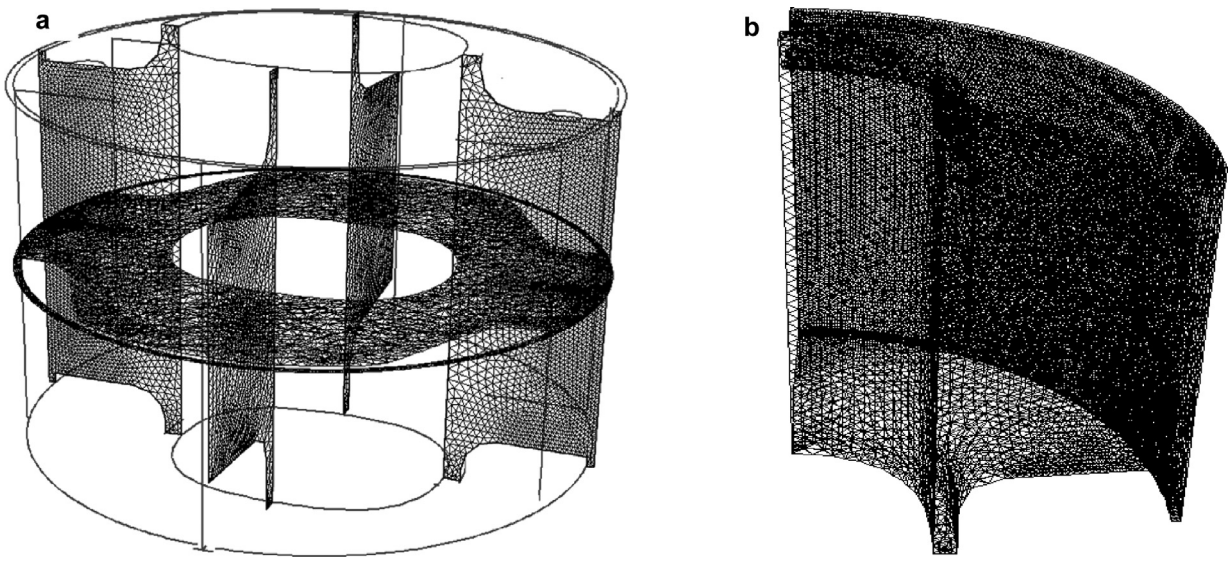

Fig. 3. Grid distribution in the computational domain, (a) on the symmetry planes, and (b) on the quarter of the model.

3.2. Boundary and initial conditions

In this study, a mass flow rate of 0.37 kg/s is imposed at the inlet boundary (the face specified by the injection point in Fig. 2) with an initial temperature of 120 °C. No-slip boundary condition with constant temperature is imposed on all solid walls. Initially, the mold cavity is filled by air and hence the volume fraction of rubber is equal to zero all over the computational domain. In order to avoid air trapping in cavity, the upper ring of the mold that is specified by "pressure outlet" in Fig. 2 is considered as outflow boundary condition for air. The main process parameters according to the injection machine specifications are given in Section 4.5.

4. Experiments

4.1. Material characterization

The required experiments are performed on a natural rubber compound provided by Partlastic Group[1] (Mashhad, Iran). This compound has a typical industrial formulation (60% NR, 35% carbon black and oil materials and 5% curing agent).

[1] http://www.partlasticgroup.com/.

Fig. 4. MDR2000 instrument made by Alpha Technologies.

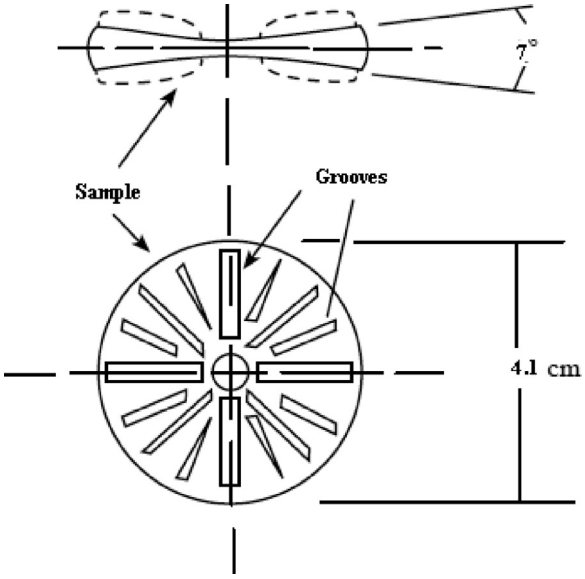

Fig. 5. Cured-sample of rubber in MDR instrument.

4.2. Rheometry tests

The Moving Die Rheometer (MDR) is an extensively used experimental tool for determination of cure curves of rubber compounds. The MDR is acknowledged to be the world standard for curemeter technology. The MDR2000 instrument made by Alpha Technologies[2], shown in Fig. 4, is capable of measuring the changes in stiffness of a rubber sample. The standard shape dimensions of the rubber sample are given in Fig. 5. The sample is located between two heated platens where the lower one oscillates sinusoidally. The MDR instrument measures the torque response of the rubber sample during its cure based on ASTM D5289. A schematic of a typical cure-curve achieved from Rheometer is shown in Fig. 6. Three main regions are specified in this figure: first, the induction: in this region the rubber sample is put into the heated cavity of the rheometer and its shear modulus drops due to softening of the compound [17]; however, the cross-links have not yet been formed.

[2] http://www.alpha-technologies.com/.

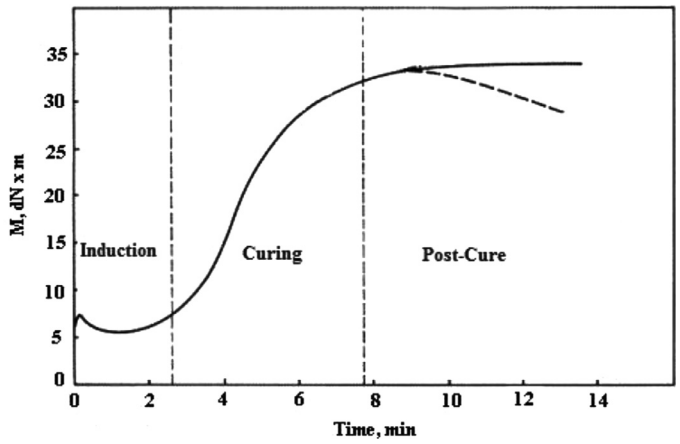

Fig. 6. Schematic of a typical cure-curve obtained from rheometer.

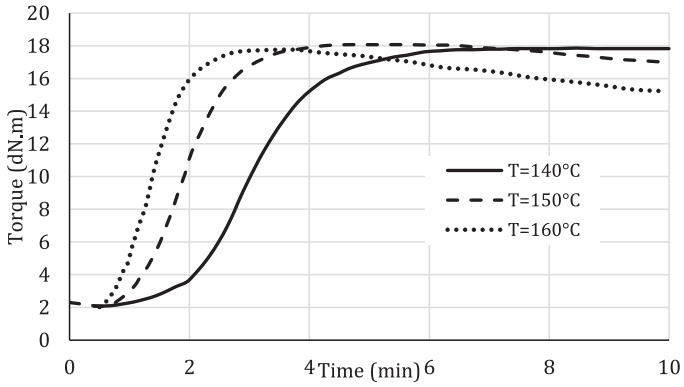

Fig. 7. Rheometry test results (torque vs. time) at different temperatures.

Table 1
The parameters of the cure model.

k_0	n	E ($\frac{J}{gmol}$)	t_0 (s)	T_0 (K)
1.37×10^{32}	4.957	358,832	2.80×10^{-11}	12,690

Next, the cure stage, where crosslinking takes place within the rubber compound. As a result of forming three dimensional cross-linked networks, the elasticity and tensile strength of the rubber is improved which results in the increasing trend of the torque curve. Finally, the post-cure, where the torque decreases or remains constant depending on the specific cure system [16]. Since the post-cure step usually has an undesirable effect on quality and physical properties of the final product, it becomes necessary to optimize the curing process [13].

The experiments in the current study are performed for various temperatures of 140, 150 and 160 °C and the resultant torque-time curves are presented in Fig. 7.

In order to convert the rheometry test results into time variations of the state of cure, the following equation is generally used [15]:

$$\alpha = \frac{M_t - M_0}{M_H - M_0} \tag{10}$$

where M_t, M_H and M_O are the instant, maximum and minimum torques, respectively. Torque-time curves can be transformed to cure kinetics curves (α versus t) using this equation, as shown in Fig. 8. The model parameters of Eqs. 5, 6 and 8 (namely, t_0, T_0, k_0 and n) could be computed by a non-linear regression. The calculated parameters are given in Table 1.

4.3. Specific heat, thermal conductivity and density of rubber

To evaluate the temperature dependent specific heat of rubber (C_p), Differential Scanning Calorimetry (DSC) measurements are performed at a fixed heating rate of 10 °C/min and temperatures of 80, 100, 140, 150 and 160 °C based on ASTM

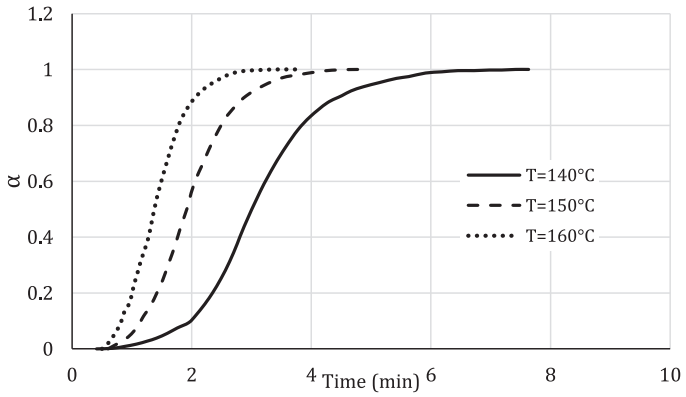

Fig. 8. Cure curves vs. time at different temperatures.

Table 2
Specific heat of rubber at different temperatures.

Temp. (°C)	80	100	140	150	160
C_p ($\frac{J}{kg.K}$)	1130	1170	1230	1250	1265

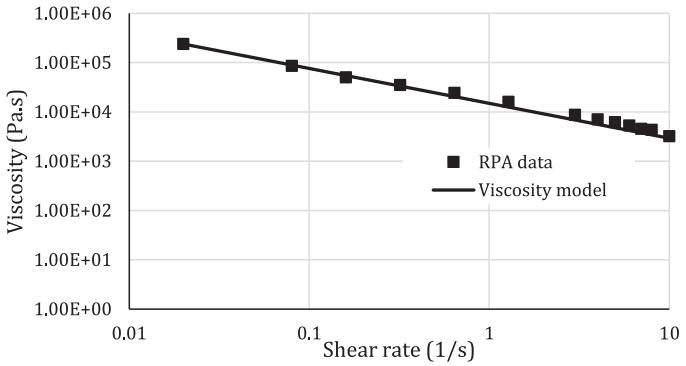

Fig. 9. Experimental measurements of viscosity as a function of the shear rate at the injection temperature.

E1269-05. The mass of the rubber samples for the non-isothermal measurements was 10 mg. The values of C_p are given in Table 2 for various temperatures.

The rubber thermal conductivity (k_t) and density (ρ) are also determined experimentally, which are 0.5 $\frac{W}{m\,^{\circ}C}$ and 1120 $\frac{kg}{m^3}$, respectively [5].

4.4. Viscometry tests

To evaluate the viscosity of rubber, viscometry tests are carried out at the injection temperature using a Rubber-Process-Analyzer (RPA) instrument of Alfa-Technologies . The experimental measurements of viscosity as a function of the shear rate are shown in Fig. 9. The constants of the non-Newtonian power law viscosity model, A and B in Eq. (4), are determined using non-linear regression analysis ($A = 5503$ kg.s$^{(B-2)}$/m and $B = 0.2929$).

4.5. Injection machine

An injection machine of Jing Day JD-RL series is used for the injection molding process. The conditions of injection process are listed in Table 3.

4.6. Mechanical compression tests

In order to estimate the best curing time for the rubber part, eight different curing times (360, 400, 410, 420, 430, 440, 450,480 s from the initial injection time) are selected and submitted to mechanical compression test in order to determine which one presents the highest stiffness, corresponding to the best curing time.

Table 3
The injection process specifications.

Injection time	Injection pressure	Injection temperature	Mold temperature
30 s	90 kg/cm^2	120 °C	160 °C

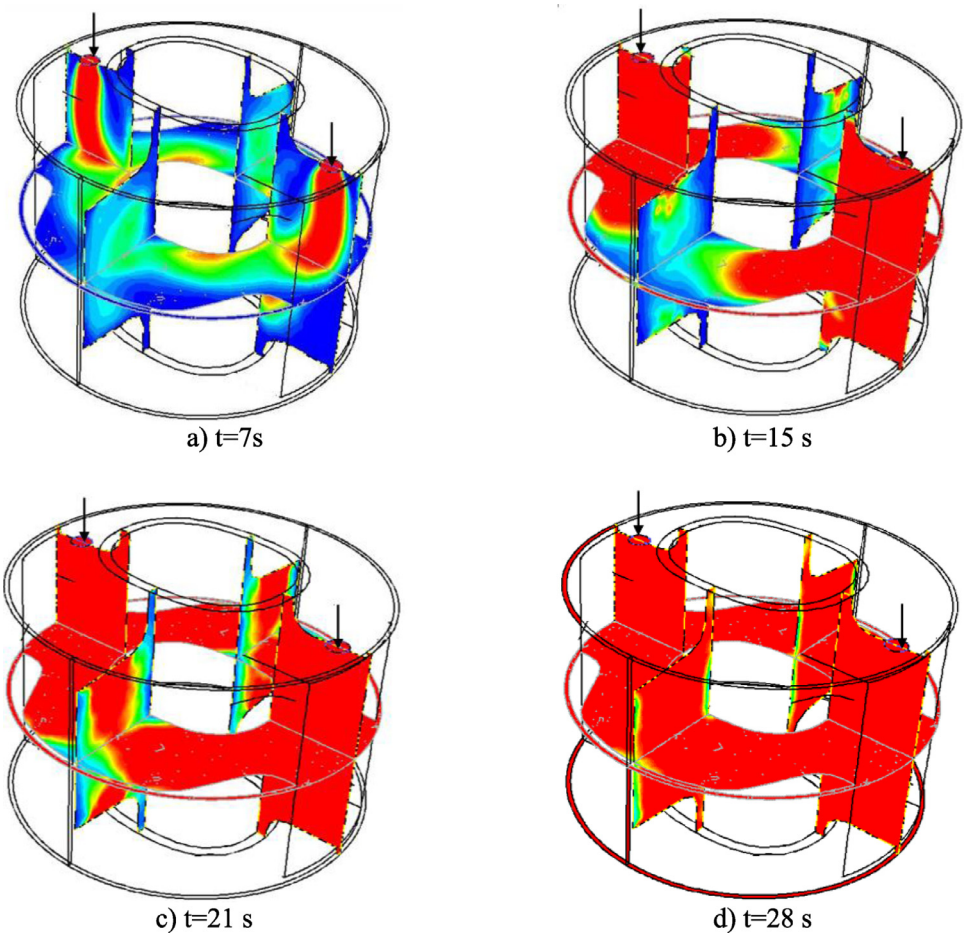

Fig. 10. The filling pattern of the rubber mold.

5. Result and discussion

In this study, a numerical simulation is presented for the curing process of a rubber article in an injection molding process using an unsteady Navier–Stokes equations solver that couples the velocity, pressure and phase composition.

The transient contours of the rubber volume fraction are shown in Fig. 10. The injection points are specified using two arrows in this figure. The filling pattern of the mold and also the filling time can be observed in this figure. The numerical filling time is 28 s which is in an acceptable agreement with the experimental filling time of 30 s obtained from the injection machine. Fig. 11 represents temperature distribution of the rubber article on a symmetry plane normal to z-direction at $t =$ 250 s. As can be seen in the figure, although 250 s have been passed from the beginning of the injection, still the rubber has not become isothermal and there is temperature gradient inside the rubber article which is due to its low thermal conductivity. The temperature history of three points inside the rubber (A, B and C in Fig. 11) with different positions relative to the mold surface is plotted in Fig. 12. As the figure shows, the points would reach the mold temperature with different trends. Such a difference in the temperature history of the rubber points, which is even more intense in thick articles, causes the material in different positions to experience different curing history. This behavior suggests that applying a kinetic model with different orders of reaction in different regions would be beneficial. In this study, a curing model has been proposed which is capable of considering a temperature dependent order of reaction.

The order of reaction, n, in Kamal model (Eq. (6)) takes a constant value; but, it can be seen from the experimental data that our model will require a temperature dependent order of reaction. Therefore, the traditional Kamal kinetic model has

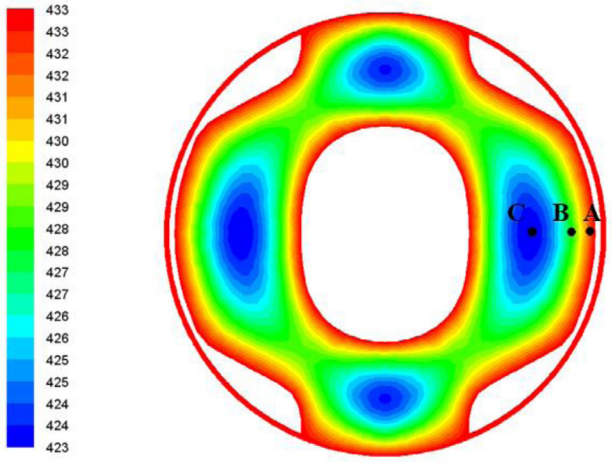

Fig. 11. Temperature distribution inside the rubber article at $t = 250$ s, (temperatures are in Kelvin).

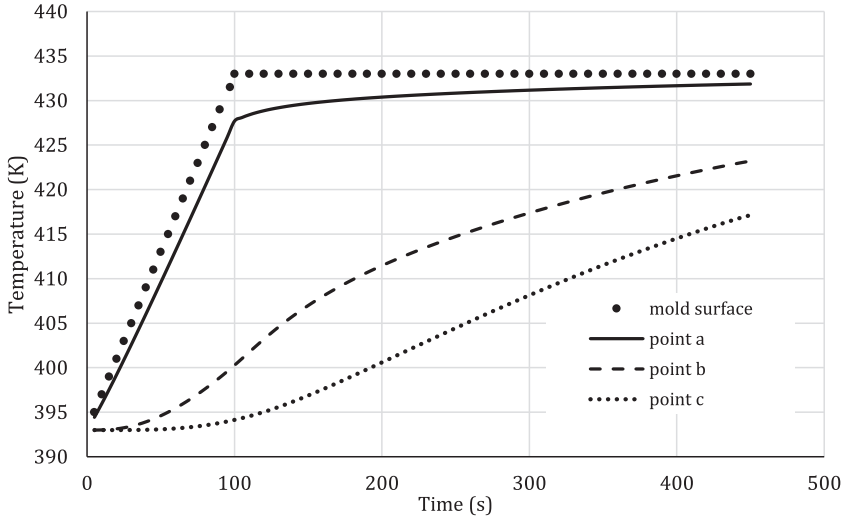

Fig. 12. Temperature history of three points inside the rubber article; The points are specified in Fig. 11.

Table 4
The constants in Eq. (12).

a	b	c
0.00212	−1.8304	3.9899

been modified in order to consider the variation of n with temperature. In this study, the order of reaction, n, in the curing kinetic model is proposed as:

$$n = aT^2 + bT + c, \tag{11}$$

where a, b and c are three material constants which are determined based on the experimental data. These constants for the experiments performed in this study are calculated using a nonlinear regression and the resultant coefficients are given in Table 4. Hence, the modified kinetic cure model would be:

$$\alpha = \frac{k.t^{aT^2+bT+c}}{1 + k.t^{aT^2+bT+c}}. \tag{12}$$

In order to verify the accuracy of the modified model, the cure-curve experimental data (using MDR at T = 155 °C) are compared with the original Kamal model and the modified Kamal model in Fig. 13. The average relative errors for the Kamal model is 16.3%, while it has reduced to 9.59% using the modified model, presented in this study.

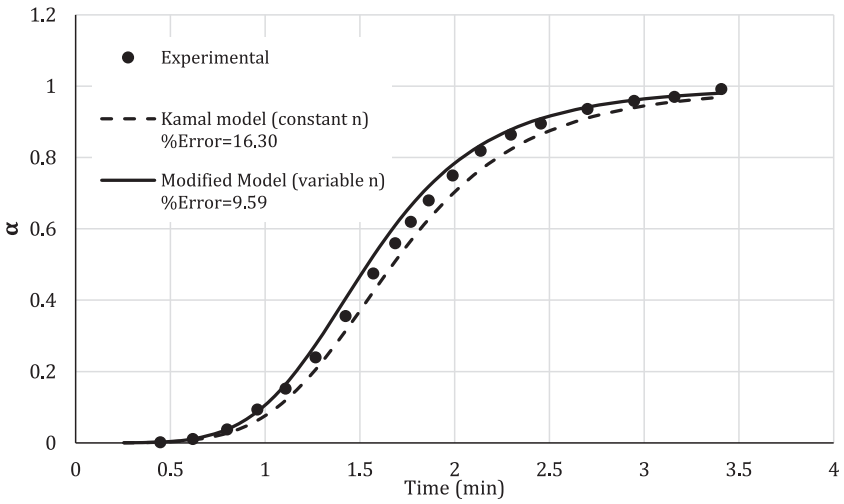

Fig. 13. Cure curves vs. time for Kamal and modified models and experimental data (MDR) at T = 155 °C.

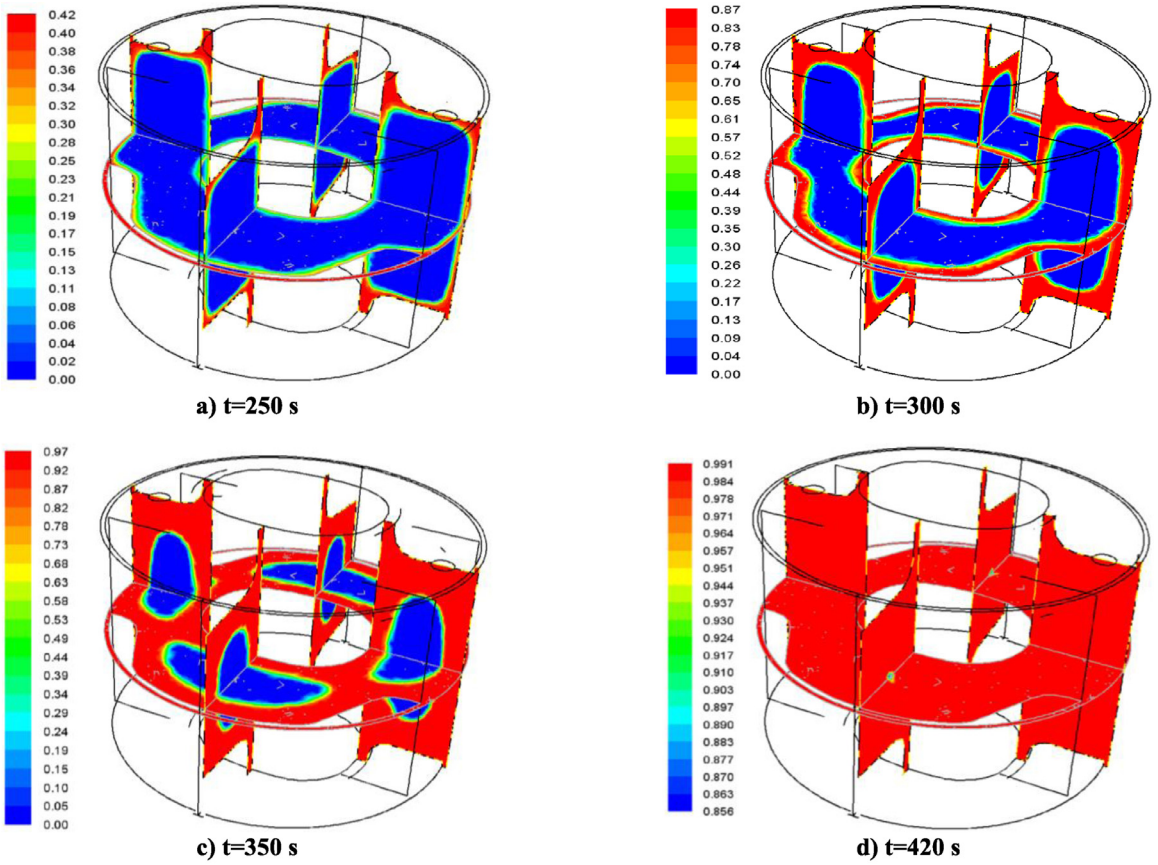

Fig. 14. The state-of-cure distributions inside the rubber article at various times.

Fig. 14 shows the state-of-cure distributions inside the rubber article at various times, obtained based on the modified Kamal model, Eq. (12). The heat dissipation from the mold walls toward the inner layers of the rubber article, plays the major role in initiating the cure reaction. As expected, the cure reaction initiates from the regions close the mold walls, due to the higher temperatures of these regions. According to Eq. (8), the non-dimensional induction time, $\bar{t}$, would reach the value of 1 in the regions with higher temperature; in other words, these regions would have a smaller induction time and the cure process starts earlier. As the figure shows, at t = 350 s, the regions close to the mold are completely cured,

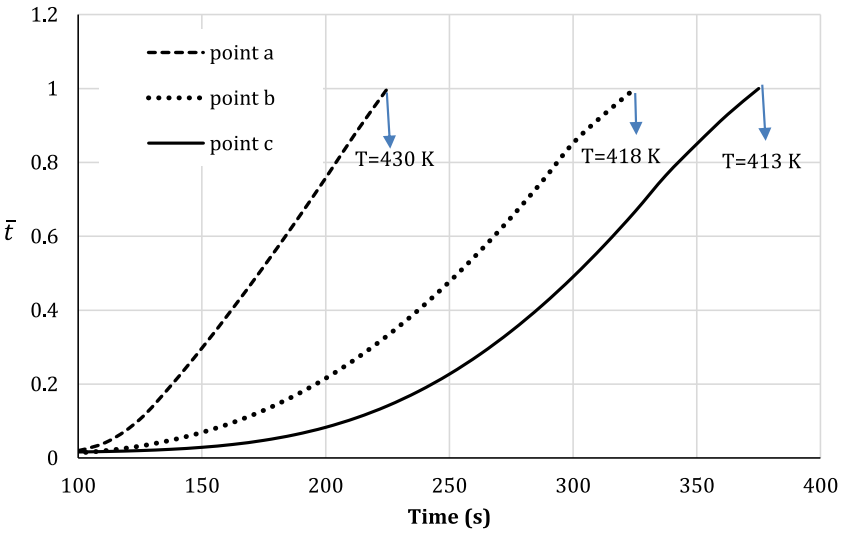

Fig. 15. Time variations of the non-dimensional induction time for the three points shown in Fig. 11.

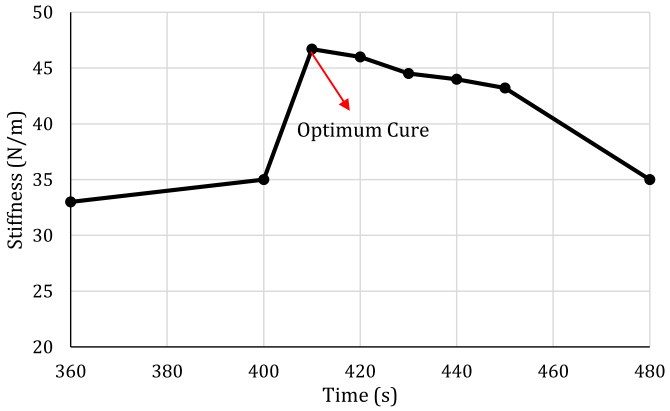

Fig. 16. Experimental values of the rubber article stiffness at various curing times.

while the non-dimensional induction time for the inner regions are still less than one. This is mainly due to the low conductivity of the rubber. The cured region, which has been formed between the mold walls and the uncured inner regions of the rubber article, acts as a thermal resistance and extends the curing time. Due to the high energy consumption of this stage, optimizing the cure time would result in a more economical process. For such thick rubber articles, typically it is not recommended to wait for the inner regions to be completed cured due to the risk of reversion of the compound close to the walls. However, for this specific product studied in this paper, slight reversion at a small region close to the walls is not so troublesome. That is because, after curing the product, the walls close to mold will be attached to a metal sheet in order to reach a higher level of reinforcement.

Fig. 15 shows the time variation of the non-dimensional induction time, $\bar{t}$, for the three points displayed in Fig. 11. The time and the temperature, at which the cure process initiates, differ for the points at different locations relative to the mold wall.

In order to determine the best curing time, eight different curing time values are selected for the experimental measurements. For each time value, the rubber article is submitted to mechanical compression tests and the stiffness of the article is measured. The resultant curve is depicted in Fig. 16. The optimum cure time is the time which corresponds to the maximum stiffness point. The figure shows that the optimum cure time occurs at $t \approx 410$ s. In order to evaluate the ability of the proposed numerical model in this study, e.g. the modified Kamal model, the time variations of the numerical state of cure obtained by each model is shown in Fig. 17. The numerical values of the state-of-cure presented in the figure, are the vertex-averaged values of α in all of the computational nodes inside the rubber. The experimental value of the optimum cure time is also specified in the figure. As can be seen, the numerical result obtained using the modified Kamal model, is in a better agreement with the experimental result.

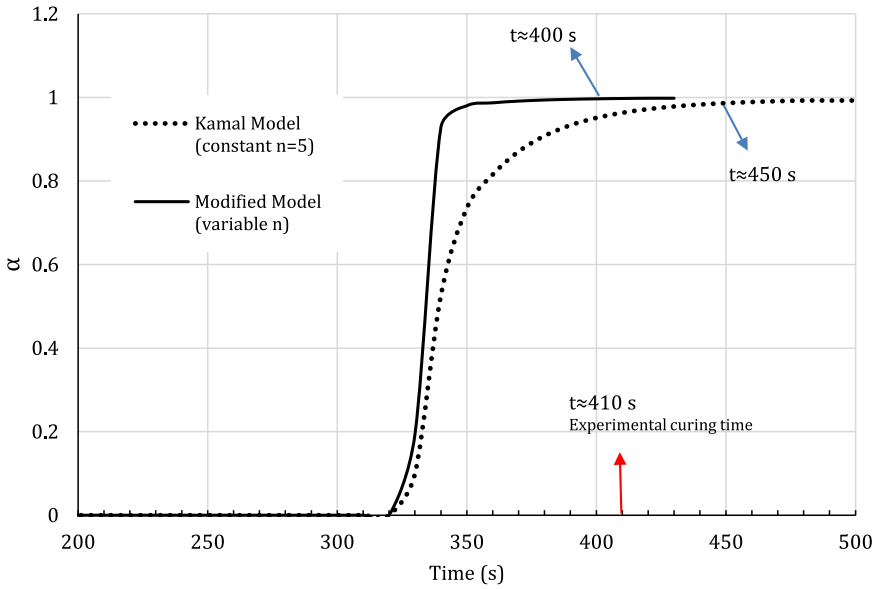

Fig. 17. Numerical curing curves obtained from the Kamal model and the Modified model.

6. Conclusions

In this study, a variable order of reaction numerical method is used for simulation of injection molding and curing process of a complex automotive rubber article. The proposed model is introduced to the Fluent 6.3.26 commercial software via a computer code written in the UDF format of the software. The applicability and accuracy of the method has been verified by comparing the calculated curing time of the rubber part with experimentally measured data. The observed satisfactory agreement between the numerical results and those of experiments revealed that the proposed method can be efficiently used to predict the optimum cure time in rubber industries.

Acknowledgment

The authors wish to express appreciation to Research Deputy of Ferdowsi University of Mashhad for supporting this project by grant No: 2/38011 04/07/94.

References

[1] J.M. Vergnad, I.D. Rosca, Rubber Curing and Properties, CRC Press, Taylor-Francis Group, New York, 2009, pp. 1–11.
[2] M.H.R. Ghoreyshi, A state-of-the-art review on the mathematical modeling and computer simulation of rubber vulcanization process, Iran Polym. J. 25 (2016) 89–109.
[3] A. Arrillaga, A.M.R. Zaldua, M. Atxurra, A.S. Farid, Techniques used for determining cure kinetics of rubber compounds, Eur. Polym. J. 43 (2007) 4783–4799.
[4] P. Ghosh, S. Katare, J.M. Caruthers, Sulfur vulcanization of natural rubber for benzothiazole accelerated, Rubber Chem. Technol. 76 (2003) 592–693.
[5] M.H.R. Ghoreishy, G. Naderi, Three-dimensional finite element modeling of rubber curing process, J. Elastom. Plast. 37 (1) (2005) 37–53.
[6] M.R. Kamal, S. Sourour, Kinetics and thermal characterisation of thermoset cure, Polym. Eng. Sci. 13 (1973) 59–64.
[7] M.H.R. Ghoreyshi, G. Naderi, Three dimensional finite element modelling of truck type curing process in mould, Iran Polym. J. 14 (2005) 735–743.
[8] G. Ramorino, M. Girardi, S. Agnelli, A. Franceschini, Injection molding of engineering rubber components: A comparison between experimental results and numerical simulation, Int. J. Mater. Form. 3 (2010) 551–554.
[9] E. Leroy, A. Souid, R. Deterre, A continuous kinetic model of rubber vulcanization predicting induction and reversion, Polym. Test. 32 (2013) 575–582.
[10] M. Rafei, M.H.R. Ghoreishy, G. Naderi, Developments of an advanced computer simulation technique for the modeling of rubber curing process, Comput. Mater. Sci. 47 (2009) 539–547.
[11] Fluent computational fluid dynamics software, Fluent v.6.3.26, theoretical manual, 2006, Fluent Inc.
[12] C. Khor, Y.Z.M. Ariff, F.C. Ani, M. Mujeebu, M.K. Abdullah, M.A. Joseph, Three-dimensional numerical and experimental investigations on polymer rheology in meso-scale injection molding, Int. Commun. Heat Mass Transf. 37 (2010) 131–139.
[13] M. Javadi, M. Moghiman, M.R. Erfanian, N. Hosseini, Numerical investigation of curing process in reaction injection molding of rubber for quality improvements, Key Eng. Mater. 462 (2011) 1206–1211.
[14] E.J. Holm, H.P. Langtangen, A unified finite element model for the injection molding process, Comput. Methods Appl. 178 (1999) 413–429.
[15] R. Ding, A.I. Leonov, A kinetic model for sulfur accelerated vulcanization of a natural rubber compound, J. Appl. Polym. Sci. 61 (1996) 455–463.
[16] P. Zhang, F. Zhao, Y. Yaun, X. Shi, S. Zhao, Network evolution based on general-purpose diene rubbers/sulfur/TBBS system during vulcanization (I), Polymer 51 (2010) 257–263.
[17] B. Karaagac, M. Inal, V. Deniz, Predicting optimum cure time of rubber compounds by means of ANFIS, Mater. Des. 35 (2012) 833–838.